Proceedings of the ASME 2010 International Design Engineering Technical Conferences & Computers and Information in Engineering Conference
IDETC/CIE 2010
August 15-18, 2010, Montreal, Quebec, Canada

DETC2010-28509

A GEOMETRIC CONSTRUCTIVE APPROACH FOR THE WORKSPACE ANALYSIS OF SYMMETRICAL 5-PRUR PARALLEL MECHANISMS (3T2R)

Mehdi Tale Masouleh *
Département de génie mécanique
Université Laval
Québec, QC, Canada, G1V 0A6
Email: mehdi.tale-masouleh.1@ulaval.ca

Mohammad Hossein Saadatzi
Faculty of Electrical & Computer Engineering
K.N. Toosi University of Technology
P.O. Box 16315-1355, Tehran, Iran
Email:saadatzi@ee.kntu.ac.ir

Clément Gosselin
Département de génie mécanique
Université Laval
Québec, QC, Canada, G1V 0A6
Email:gosselin@gmc.ulaval.ca

Hamid D. Taghirad
Faculty of Electrical & Computer Engineering
K.N. Toosi University of Technology
P.O. Box 16315-1355, Tehran, Iran
Email:Taghirad@kntu.ac.ir

ABSTRACT

This paper investigates an important kinematic property, the constant-orientation workspace, of five-degree-of-freedom parallel mechanisms generating the 3T2R motion and comprising five identical limbs of the PRUR type. The general mechanism originates from the type synthesis performed for symmetrical 5-DOF parallel mechanism. In this study, the emphasis is placed on the determination of constant-orientation workspace using geometrical interpretation of the so-called vertex space, i.e., motion generated by a limb for a given orientation, rather than relying on classical recipes, such as discretization methods. For the sake of better understanding a CAD model is also provided for the vertex space. The constructive geometric approach presented in this paper provides some insight into the architecture optimization. Moreover, this approach facilitates the computation of the evolution of the volume of the constant-orientation workspace for different orientations of the end-effector.

*Address all correspondence to this author.

INTRODUCTION

Parallel mechanisms, often erroneously said to be recent developments, have a pedigree far more ancient than that of the serial robot-arms which are usually called *anthropomorphic* [1]. The tripod, used by photographers, can be regarded as a precursor which comprises a small triangular platform with three supporting adjustable legs. A comprehensive survey about the true origins of parallel mechanisms is elaborated in [2]. Over the past two decades, parallel mechanisms evolved from the rather marginal mechanisms, such as the centuries-old tripod, to widely used mechanical architectures which become the state of the art of the commercial world, for instance *Gough-Stewart* platform and *Delta* robot [3]. For a long time, parallel mechanisms, due to some remarkable kinematic properties, have stimulated the interest of researchers and industries and they have been extensively synthesized using intuition and ingenuity. Recently, a systematic approach has been developed, namely the *Type synthesis* [3], which opens some avenues to list all possible kinematic arrangements for a specific motion pattern.

The development of type synthesis channels researchers to synthesize parallel mechanisms with fewer than six–degrees–

of–freedom (DOF), referred to as lower mobility mechanisms, since it was believed that parallel mechanisms with identical limb structures, topologically symmetrical, with 4 and 5-DOF cannot be built. Thus, as far as 5-DOF mechanisms with identical limb structures are concerned, researchers have mainly worked on the type synthesis [3–8]. It is worth noticing that most existing 5-DOF parallel manipulators are built using a 5-DOF passive leg which constrains some actuated 6-DOF limbs [9, 10].

Five-DOF parallel mechanisms are a class of parallel mechanisms with reduced DOFs which, according to their mobility, fall into three classes: (1) three translational and two rotational freedoms (3T2R), (2) three rotational and two planar translational freedoms ($3R2T_p$) and (3) three rotational and two spherical translational freedoms ($3R2T_s$) [3]. Since, in the industrial context, the 3T2R motion can cover a wide range of applications including, among others, 5-axis machine tools and welding, therefore, in this research, the kinematic properties of this class will be investigated. Recently, the machine tool industry has discovered the potential advantages of parallel mechanisms and many parallel machine tools have been developed based on either the 6-DOF parallel mechanisms (Traditional "Gough-Stewart platform") or asymmetrical 5-DOF parallel mechanisms in which a passive leg constrains the motion of the end-effector [11]. For a comprehensive list of the so-called parallel machine tools in industrial context see [2, 11].

To the best knowledge of the authors, up to now, very few kinematic studies have been conducted on symmetrical 5-DOF parallel mechanisms [12]. This is probably due to their short history. Recently, in [13–15] some kinematic properties, such as singular configurations, of certain 5–DOF symmetrical 3R2T parallel mechanisms have been studied. However, the kinematic properties of symmetrical 5-DOF performing 3T2R motion pattern are still not well understood and there are many issues which should inevitably be addressed including the constant-orientation workspace.

Parallel mechanisms are well-known to have a restricted workspace compared to their counterpart, serial manipulators. Thus a thorough analysis of the workspace of parallel mechanisms is primordial before entering into their design stage. Various approaches are proposed in the literature to obtain the workspace of parallel mechanisms [16]. According to which type of mobilities set, translational or rotational, is fixed, different types of workspace are possible. The focus of this paper is on the one that is often used: constant-orientation workspace. Generally, classical recipes, such as discretization algorithms and node search approach, are used by most researchers which can be applied to any kind of parallel mechanisms. The main drawback of such approaches is that they are computationally intensive and consequently time consuming to run in a computer system. To overcome such a problem, instead of treating numerically the constant-orientation workspace, the problem is investigated geometrically which is called the *geometrical constructive approach*. The central concept of the latter approach is based on the identification of the curves, surfaces and volumes that are obtained by successively releasing the joints from the base to the platform and formulating mathematically. In this paper, the geometrical constructive approach is used which is inspired from the method proposed in [17, 18] for the computation of the constant-orientation workspace of 6-DOF Gough-Stewart platform. Moreover, the topology of the vertex space, constant-orientation workspace of one limb, is obtained and modeled in a CAD system which results in the CAD model of the constant-orientation workspace.

The remainder of this paper is organized as follows. The architecture and the general kinematic properties of the 5-PRUR parallel mechanism which originated from the type synthesis performed in [3, 7] are first outlined. The IKP is addressed and two general classes for 5-PRUR arrangement are proposed. The constant-orientation workspace is interpreted geometrically and the results are implemented in a CAD system. Moreover, an algorithm, inspired from the one presented in [17] for the general 6–DOF Stewart platform, is proposed for computing the boundary of the constant-orientation workspace. Based on the latter algorithm, the volume of the constant-orientation workspace is obtained and plotted with respect to the two permitted rotational DOFs.

1 ARCHITECTURE REVIEW AND KINEMATIC MODELING OF 5-PRUR

Figures 1 and 2 provide respectively representations of two possible arrangements for a PRUR limb and a CAD model for a 5-DOF parallel mechanism, called *Pentapteron* which was first revealed in [19]. Pentapteron is an orthogonal 5-DOF parallel mechanism arising from the type synthesis presented in [3, 7] and consists of 5 legs of the PRUR type linking the base to a common platform. Such a mechanism can be used to produce all three translational DOFs, plus two independent rotational DOFs (3T2R) of the end-effector, namely (x, y, z, ϕ, θ). In the latter notation, (x, y, z) represent the translational DOFs with respect to the fixed frame O, illustrated in Fig. 2, and (ϕ, θ) stand respectively for the orientation DOFs around axes x and y. From the type synthesis presented in [7], the geometric characteristics associated with the components of each leg of type PRRRR are as follows: The five revolute joints attached to the platform (the last R joint in each of the legs) have parallel axes, the five revolute joints attached to the base have parallel axes, the first two revolute joints of each leg have parallel axes and the last two revolute joints of each leg have parallel axes. It should be noted that the second and third revolute joints in each leg are built with intersecting and perpendicular axes and are thus assimilated to U (Universal) joints. In addition, the axes of the first R joints in all the legs are arranged to be parallel to the direction of a group of two of the linearly actuated joints. Therefore, two types of

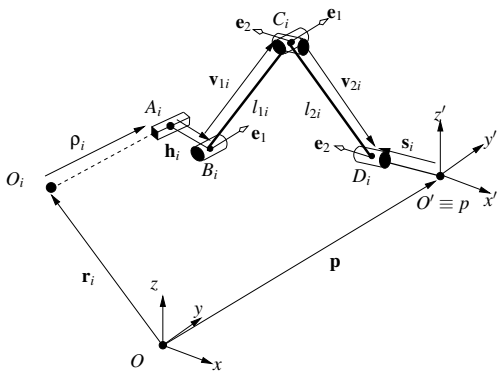

(a) $\underline{\text{C}}\text{UR} \equiv \Gamma = 1$

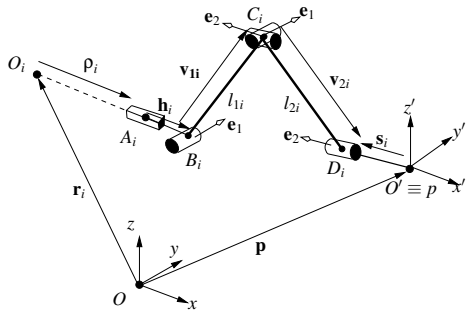

(b) $\underline{\text{P}}\text{RUR} \equiv \Gamma = 0$

Figure 1. SCHEMATIC REPRESENTATION OF, (A) $\underline{\text{P}}$RUR AND (B) $\underline{\text{C}}$UR.

kinematic arrangements are possible, as depicted in Fig. 1, for the legs: a) the parallel type, Fig. 1(a), and the perpendicular type, Fig. 1(b). In fact, $\Gamma = 0$ and $\Gamma = 1$ differ in some kinematic properties such as constant-orientation workspace and the Inverse Kinematic Problem (IKP) formulation. It is noted that Γ designates the cosine of the angle between the prismatic actuator axis and the first R joint axis.

The rotation from the fixed frame O_{xyz} to the moving frame $O'_{x'y'z'}$ is defined as follows: a first rotation of angle ϕ is performed around the $x-$ axis followed by the second rotation about the $y-$ axis by angle θ. The latter leads to the following rotation matrix:

$$\mathbf{Q} = \begin{bmatrix} \cos\theta & \sin\phi\sin\theta & \cos\phi\sin\theta \\ 0 & \cos\phi & -\sin\phi \\ -\sin\theta & \sin\phi\cos\theta & \cos\phi\cos\theta \end{bmatrix}. \qquad (1)$$

In this paper the superscript $'$ for a vector stands for its representation in the mobile frame. In a 5-$\underline{\text{P}}$RUR parallel mechanism, the axes of all the R joints are always parallel to a plane defined by its normal vector $\mathbf{e}_3 = \mathbf{e}_1 \times \mathbf{e}_2$ where $\mathbf{e}_1$ and $\mathbf{e}_2$ are unit vectors defining the direction of R joints. From *screw theory* [1], it follows that the mechanism has no possibility to perform a rotation about an axis which is orthogonal to a plane spanned by $[\mathbf{e}_1, \mathbf{e}_2]$.

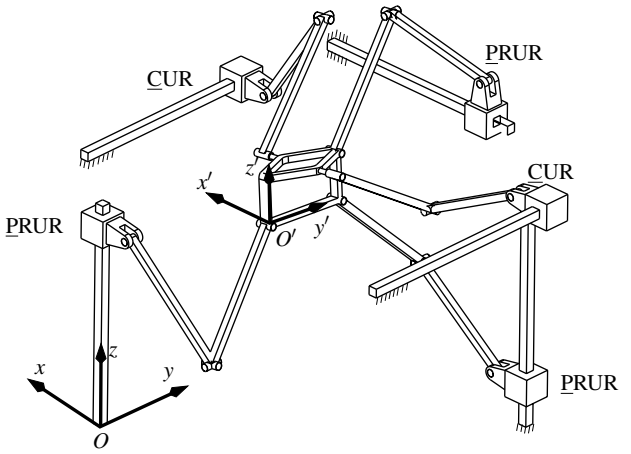

Figure 2. CAD MODEL OF PENTAPTERON A 5-DOF(3T2R) PARALLEL MECHANISM

2 INVERSE KINEMATIC PROBLEM (IKP)

The IKP pertains to finding the set of actuated joint variables for a given pose (position and orientation) of the platform. In the i^{th} leg, the motion of the actuated prismatic joint is measured with respect to a reference point A_i, located on the axis of the prismatic actuator. Vector $\mathbf{e}_{r_i}$ is in turn defined as a unit vector in the direction of the prismatic joint and therefore the vector connecting point O_i to point A_i can be written as $\rho_i = \rho_i \mathbf{e}_{r_i}$. Vector $\mathbf{r}_i$ is defined as the position vector of point O_i, the starting point of the prismatic actuator, in the fixed reference frame. Similarly, vector $\mathbf{s}_i$ is the vector connecting point O' of the platform to a reference point D_i on the axis of the last revolute joint of the i^{th} leg. Point C_i is defined as the intersection of the axes of the second and third revolute joints of the i^{th} leg. Vectors $\mathbf{v}_{1i}$ and $\mathbf{v}_{2i}$ are respectively the vector connecting point B_i to point C_i and point C_i to D_i. Since in the proposed architecture vectors $\mathbf{e}_1$ and $\mathbf{e}_2$ are orthogonal, one has: $\mathbf{e}_1 \cdot \mathbf{e}_2 = 0$. Finally, the position of the platform is represented by vector $\mathbf{p} = [x, y, z]^T$ connecting point O to point O' and the orientation of the moving frame with respect to the fixed frame is given by a rotation matrix $\mathbf{Q}$. For a given value of the angles ϕ and θ, matrix $\mathbf{Q}$ is readily computed and vectors $\mathbf{s}_i$ and $\mathbf{e}_2$ are then obtained as:

$$\mathbf{s}_i = \mathbf{Q}\mathbf{s}'_i, \qquad \mathbf{e}_2 = \mathbf{Q}\mathbf{e}'_2 = [\cos\theta, 0, -\sin\theta]^T. \qquad (2)$$

With reference to Fig. 1, the following equations, arising from the kinematic constraint of the i^{th} limb, can be written:

$$(x_{Ci}-x_{Bi})^2+(z_{Ci}-z_{Bi})^2=l_{1i}^2 \tag{3}$$
$$(x_{Di}-x_{Ci})^2+(y_{Di}-y_{Ci})^2+(z_{Di}-z_{Ci})^2=l_{2i}^2 \tag{4}$$
$$(x_{Di}-x_{Ci})\cos\theta-(z_{Di}-z_{Ci})\sin\theta=0 \tag{5}$$

such that the first two equations represent, respectively, the magnitude of $\mathbf{v}_{1i}$ and $\mathbf{v}_{2i}$ and the last one corresponds to the kinematic constraints between $\mathbf{e}_2$ and $\mathbf{v}_{2i}$, i.e., $\mathbf{e}_2 \perp \mathbf{v}_{2i}$. The solution for the IKP is quite different for each case, i.e., $\Gamma=1$ and $\Gamma=0$, and requires to be investigated separately.

2.1 IKP for PRUR $\equiv(\Gamma=0)$

Let us consider the case for which the prismatic actuator is along x axes, which is denoted as ${}^{x}\rho_i$. As it can be observed, the latter expressions contains passive variables, $C_i(x_{Ci}, y_{Ci}, z_{Ci})$ and $D_i(x_{Di}, y_{Di}, z_{Di})$, which are respectively the coordinates of the passive U joint and the R joint attached to the platform. Using the fact the the last R joint is attached to the platform, the coordinate of point D_i can be related to the pose of the platform. One has: $[x_{Di},\ y_{Di},\ z_{Di}]^T=\mathbf{p}+\mathbf{Q}\mathbf{s}'_i$. Upon eliminating the above passive variables and by skipping mathematical details, leads to the following for the IKP:

$$\begin{aligned}{}^{x}\rho_i =& x_{Di}+(-1)^m\sin\theta\sqrt{\mathcal{K}_i}\\ &+(-1)^n\sqrt{l_{1i}^2-(z_{Di}+(-1)^m\cos\theta\sqrt{\mathcal{K}_i}-z_{Bi})^2}\end{aligned} \tag{6}$$

where $\mathcal{K}_i=l_{2i}^2-(y_{Di}-y_{Ci})^2$. Moreover, $m=\{0,1\}$ and $n=\{0,1\}$ stand for different working modes where it follows that the IKP admits up to four solutions. An analogous approach leads to obtain the IKP when the prismatic actuator is along z axis:

$$\begin{aligned}{}^{z}\rho_i =& z_{Di}+(-1)^m\cos\theta\sqrt{\mathcal{K}_i}\\ &+(-1)^n\sqrt{l_{1i}^2-(x_{Di}+(-1)^m\sin\theta\sqrt{\mathcal{K}_i}-x_{Bi})^2}\end{aligned} \tag{7}$$

2.2 IKP for CUR $\equiv(\Gamma=1)$

In this case, Eqs. (3-5) should be solved for $y_{Ci}=\rho_i$ for a given pose of the platform. Having in mind that $y_{Ci}=y_{Bi}=\rho_i$, the coordinates of point C_i are unknown for the IKP. Thus by eliminating passive variables, and skipping mathematical details, it follows that IKP formulation can be divided into two expressions for two different sets of working modes:

$${}^{1}_{p}\rho_i=y_{Di}+(-1)^p\sqrt{l_{2i}^2-({}^{1}\mathcal{K}'_i)^2} \tag{8}$$
$${}^{2}_{p}\rho_i=y_{Di}+(-1)^p\sqrt{l_{2i}^2-({}^{2}\mathcal{K}'_i)^2} \tag{9}$$

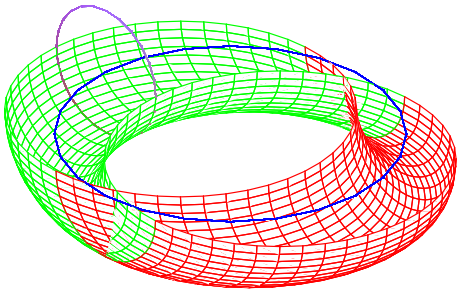

Figure 3. THE LOWER HALF OF A BOHEMIAN DOME. THE REPRESENTATION IS ADAPTED FROM [18].

where

$${}^{1}\mathcal{K}'_i=|\mathbf{v}_i\cdot\mathbf{e}_3|-\sqrt{l_{1i}^2-(\mathbf{v}_i\cdot\mathbf{e}_2)^2}\quad {}^{2}\mathcal{K}'_i=|\mathbf{v}_i\cdot\mathbf{e}_3|+\sqrt{l_{1i}^2-(\mathbf{v}_i\cdot\mathbf{e}_2)^2} \tag{10}$$

so that $p=\{0,1\}$. From the above expressions it can be deduced that the IKP admits up to four solutions.

3 WORKSPACE ANALYSIS

The complete workspace of the 5-RPUR manipulator can be regarded as a five–dimensional space for which no visualization exists. In the context of parallel mechanism workspace, one representation that is often used is *the constant-orientation workspace*, which is the set of locations of the moving platform that can be reached with a given prescribed orientation [16]. In this paper, the passive joints are considered to have an unrestricted excursion range. Moreover, the mechanical interferences are not considered in the workspace analysis. Geometrically, the problem of determining the constant-orientation workspace for a limb of the 5-PRUR parallel mechanism can be regarded as follows: For a fixed elongation of the prismatic actuator, the first revolute joint provides a circular trajectory centred at A_i with l_{1i} as radius. The second link generates a surface by sweeping a second circle, with $\mathbf{e}_2$ as axis and l_{2i} as radius, along the first circle. Since the direction of $\mathbf{e}_2$ is prescribed and must remain constant, such a surface generates a quadratic surface and is called a *Bohemian dome*. This quadratic surface can be obtained by moving a circle that remains parallel to a plane along a curve that is perpendicular to the same plane, as shown in Fig. 3. Once this surface is obtained, it should be extended in such a way that represents the vertex space of the limb for different elongations of the prismatic actuators with respect to its stroke $\Delta\rho_i=\rho_{i\max}-\rho_{i\min}$. The main challenge in obtaining the topology of the vertex space is to find a general and complete model to extend the Bohemian dome to the vertex space. As mentioned above, $\Gamma=0$ and $\Gamma=1$ have different vertex spaces. Moreover, the vertex space of each case falls into different classes depending on the values of l_{1i}, l_{2i} and $\Delta\rho_i$. In what concerns the rotational parameters, (ϕ,θ), only

θ influences the vertex space topology. The influences of l_{1i}, l_{2i}, $\Delta\rho_i$ and θ on the vertex space are the main reasons that make it difficult to assess geometrically the vertex space of a PRUR limb and for which it requires a thorough and comprehensive analysis. In the following section, first, the topology of the vertex space, for both cases $\Gamma = \{0,1\}$, is elaborated and then the constant-orientation workspace is investigated. It is worth noticing that the study of both vertex spaces and constant-orientation workspace are conducted by using a CAD model and also a constructive geometric approach inspired from the one proposed in [17].

3.1 Topology of the Vertex Space

Prior to finding the constant-orientation workspace, the topology of the vertex space generated by both types of PRUR limb, i.e., $\Gamma = \{0,1\}$, is presented. As mentioned above, among the DOFs of the platform only θ influences the shape of vertex space. Before presenting the details related to the construction of the CAD model of the vertex space, the complexity of the model is discussed briefly. In fact, θ is the rotation angle around axis $\mathbf{e}_1$, which is in direction of y axis. Thus in the case for which the prismatic actuator is along the y axis, i.e., $\Gamma = 1$, the vertex space for different angles of θ can be obtained by applying a rotation around the prismatic actuators axis by θ. It is apparent that the latter rotation preserves the direction of the prismatic actuators. Thus for $\Gamma = 1$ once the vertex space for $\theta = 0$ is in hand then it can be readily extended for different θ. By contrast, the vertex space of $\Gamma = 0$ cannot be modeled readily in such a way that covers different θ since rotating the vertex space obtained for $\theta = 0$ for $\Gamma = 0$ around $\mathbf{e}_1$ does not preserve the direction of the prismatic actuator. In what concerns the second alternative toward obtaining the boundary of the vertex space, a geometrical constructive approach is used.

3.1.1 Topology of the Vertex Space for $\Gamma = 1$.

Two distinct types of holes can appear in the Bohemian dome with $\Gamma = 1$, depending on the geometric parameters of the constituting circles: a throughout hole and a side hole, called respectively $\mathcal{H}_1$ and $\mathcal{H}_2$, which are due to:

1. $\mathcal{H}_1$: when $\Delta\rho_i < l_{2i}$
2. $\mathcal{H}_2$: when $l_{2i} < l_{1i}$

Thus, from the above, the topology of the vertex space for $\Gamma = 1$ falls into four cases:

1. Γ_{01}: $\Delta\rho_i \geq l_{2i}$ and $l_{2i} \geq l_{1i}$, none of the holes;
2. Γ_{02}: $\Delta\rho_i \geq l_{2i}$ and $l_{2i} \leq l_{1i}$, just $\mathcal{H}_2$;
3. Γ_{03}: $\Delta\rho_i < l_{2i}$ and $l_{2i} \geq l_{1i}$, just $\mathcal{H}_1$;
4. Γ_{04}: $\Delta\rho_i < l_{2i}$ and $l_{2i} < l_{1i}$, both $\mathcal{H}_1$ and $\mathcal{H}_2$.

Figure 4 demonstrates the four different vertex spaces belonging to $\Gamma = 1$. From the latter figure it can observed how $\mathcal{H}_1$ and $\mathcal{H}_2$ may influence vertex space. It can be readily deduced that an optimal design for a $\Gamma = 1$ corresponds to Γ_{01}. All the vertex spaces depicted in Fig. 4 correspond to a configuration for which $\theta = 0$. As mentioned previously, vertex spaces for different values of θ for $\Gamma = 1$ can be obtained by applying a rotation about the axis of the prismatic actuator by θ.

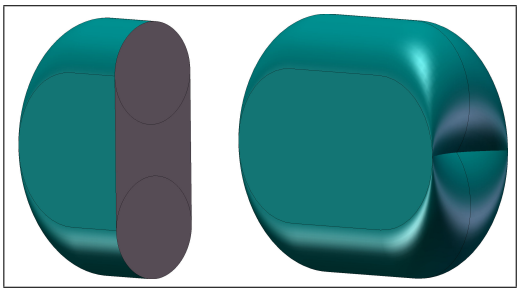

(a) Γ_{01}

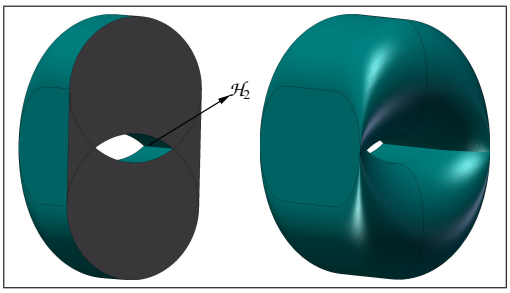

(b) Γ_{02}

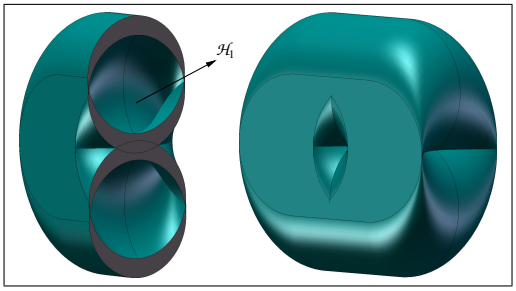

(c) Γ_{03}

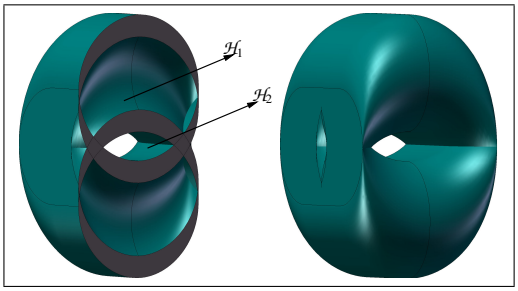

(d) Γ_{04}

Figure 4. CAD MODEL OF THE VERTEX SPACE FOR Γ_{0I}, $I = 1,\ldots,4$.

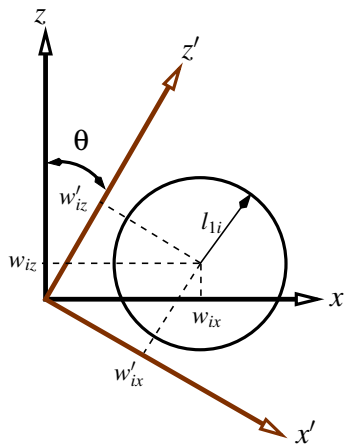

Figure 5. BOUNDARY GENERATED BY THE FIRST MOVING LINK FOR $\Gamma = 1$.

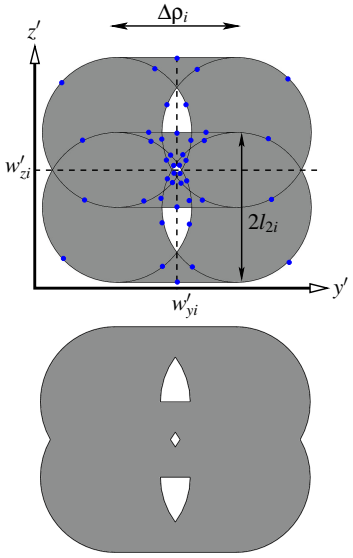

Figure 6. BOUNDARY GENERATED BY THE SECOND MOVING LINK FOR $\Gamma = 1$ DUE TO THE MOTION GENERATED BY THE FIRST MOVING LINK.

For the remaining of this subsection we attempt to obtain the vertex space by exploring the IKP and the geometrical characteristics of $\Gamma = 1$ which will be helpful later on for the geometrical construction of the constant-orientation workspace. Since in this case we are dealing with a three dimensional space, a cross sectional plane should be considered in order to reduce the problem to a two dimensional one. From a geometrical inspection, it follows that a cross sectional plane, called $\mathcal{X}$, which is rotated around the y-axis of the fixed frame by angle θ results in a homogeneous section for vertex space and leads to conventional geometric objects such as circles and lines. This helps to reduce the complexity of the computation and, to be precise, leads to an algorithm which consists in finding the intersection of some known geometric objects such as intersections of circles and lines. In the fixed frame, the vertex space, $\mathbf{w}_i$, can be formulated mathematically as follows:

$$\mathbf{w}_i = \mathbf{r}_i - \mathbf{Q}\mathbf{s}'_i \tag{11}$$

The particular cross section $\mathcal{X}$ defined above, implies that the above expression should be multiplied by $\mathbf{Q}_{y,\theta}^{-1}$ where $\mathbf{Q}_{y,\theta}$ stands for the rotation around the y-axis by angles θ:

$$\mathbf{w}'_i = \mathbf{Q}_{y,\theta}^{-1}\mathbf{w}_i = \mathbf{Q}_{y,\theta}^{-1}\mathbf{r}_i - \mathbf{Q}_{x,\phi}\mathbf{s}'_i \tag{12}$$

where $\mathbf{Q}_{x,\phi}$ represents the rotation matrix around the x-axis by angles ϕ. In the above one should be aware that $\mathbf{Q} = \mathbf{Q}_{y,\theta}\mathbf{Q}_{x,\phi}$ which is coming from the rotation sequence order. Each limb is constituted of two moving links and their corresponding motions are shown respectively in Figs. 5 and 6. From Fig. 5 it follows that:

$$(z' - w'_{iz})^2 + (x' - w'_{ix})^2 = l_{1i}^2 \tag{13}$$

where $\mathbf{w}' = [w'_{ix}, w'_{iy}, w'_{iz}]$. The cross section is followed along the x'-axis. Thus, for a given $x' = x_H$, two solutions are in hand for z', called z'_{bj}, $j = \{1,2\}$, which are the z' coordinates of two set of circles in Fig. 6. The equation representing the four circles in Fig. 6 can be expressed as follows:

$${}^1\mathcal{C}_i: \quad (z' - z'_{bj})^2 + (y' - w'_{iy} \pm \frac{\Delta\rho_i}{2})^2 = l_{2i}^2, \quad j = 1,2 \tag{14}$$

Referring to Fig. 6, the expression of the four lines, called $\mathcal{L}_i$, tangent to the above circles having zero slopes is:

$${}^1\mathcal{L}_i: \quad z'_{bj} \pm l_{2i} \tag{15}$$

The intervals of the vertex space are as follows:

$$\lim_{\min i} x : w'_{ix} - l_{1i} \leq x'_H \leq w'_{ix} + l_{1i} : \lim_{\max i} x \tag{16}$$

$$w_{iy} - l_{2i} - \frac{\Delta\rho_i}{2} \leq y'_H \leq w_{iy} + l_{2i} + \frac{\Delta\rho_i}{2} \tag{17}$$

$$w_{ix} - l_{1i} \leq z'_H \leq w_{iz} + l_{1i} \tag{18}$$

for which the cross section should be repeated with respect to Eqn. (16). For which $[x'_H, y'_H, z'_H]$ stands for the coordinates of

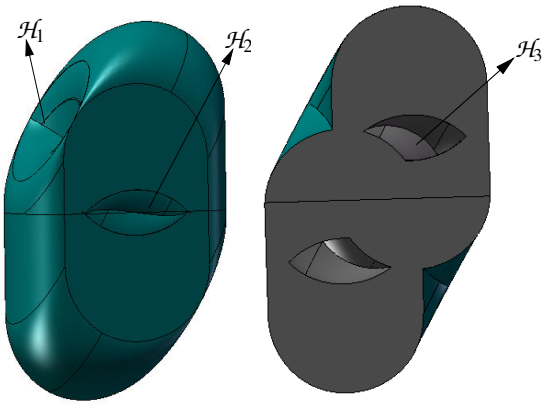

Figure 7. CAD MODEL OF THE VERTEX SPACE OF $\Gamma = 0$ FOR $\theta = \frac{\pi}{6}$.

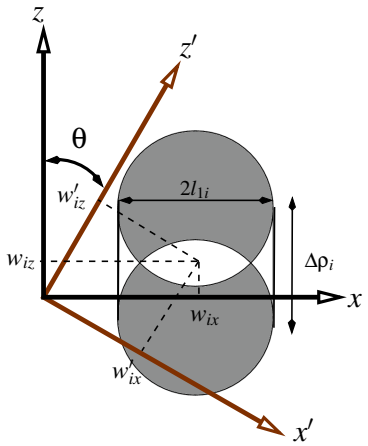

Figure 8. BOUNDARY GENERATED BY THE FIRST MOVING LINK FOR $\Gamma = 0$.

the cross section. As it can be deduced from Fig. 6, the problem of obtaining the vertex space for $\Gamma = 1$ is made equivalent to finding the intersections of the four circles connect by four lines, Eqs. (14) and (15), for a given cross section $\mathcal{X}$, with respect of the interval given in Eqs. (16-18) and, finally, identifying which intersection is constituting the boundary of the vertex space. To do so, we resort to the algorithm presented in [17]. The foregoing algorithm is not fully developed here. Thus the last step consists in obtaining all the circular arcs and lines defined by the intersection points found above and ordering these points. This should be accompanied by a checking procedure to identify the arcs and lines that constitute the boundary of the workspace. To do so, for a given curve(line or circle portion), belonging to a given arc a point lying on the curve is chosen, preferably not one of the end points. Then, using the IKP, it is verified whether this point has *boundary condition* which means that a little variation on this point leads to violate either the constraint inequalities of the IKP or the strokes of the prismatic actuator. Since a CAD model is presented for the vertex space of $\Gamma = 1$ thus the vertex space obtained by using the above procedure is omitted. However, the above formulation will be used for obtaining the constructive geometric analysis of constant-orientation workspace.

3.1.2 Topology of the Vertex Space for $\Gamma = 0$. The vertex space generated by a PRUR limb having a prismatic actuator along $x-$ axis is equivalent to the vertex space generated by the same leg having the prismatic actuators along z-axis but rotated by $\frac{\pi}{2}$ around the axis of the prismatic actuator. Thus, only the vertex space for limb with prismatic actuator in the direction of z axis is elaborated.

In the case of $\Gamma = 0$, the topology of the vertex space is highly related to θ in such a way that the vertex space for $\theta = 0$ could not be extended to other θ by a simple rotation. Moreover, for different θ the shape and characteristic of the holes vary. In this paper the complete instructions are not given for obtaining the vertex space of $\Gamma = 0$ and will be the subject of an upcoming publication. However some general outlines are given. In contrast of $\Gamma = 1$, in the case of $\Gamma = 0$, there are three types of holes:

1. $\mathcal{H}_1$: Always exists, except for $\theta = 0, \pi$. This hole is overall with respect of the following condition:
   if $(l_{1i}\cos\theta - \Delta\rho_i \sin\theta) > 0$ the condition becomes: $l_{2i} > \sqrt{l_{1i}^2 - \left(\frac{\Delta\rho_i}{2}\right)^2} - \frac{\Delta\rho_i}{2}\cos\theta$;
   otherwise, the condition is: $l_{2i} > \frac{l_{1i}}{\sin\theta}$.
2. $\mathcal{H}_2$ and $\mathcal{H}_3$ exist when $\Delta\rho_i < 2l_{1i}$:
   $\mathcal{H}_2$ is overall when: $\frac{l_{1i}\sin(\theta-\beta)}{\sin\theta} < l_{2i}$ where $\beta = \arcsin\left(\frac{\Delta\rho_i \sin\theta}{2l_{1i}}\right)$;
   $\mathcal{H}_3$ is not overall but it would be larger when $\Delta\rho_i$ decreases.

Figure (7) represents the CAD model of the vertex space for a limb with $l_{1i} = 100$, $l_{2i} = 90$ and $\Delta\rho_i = 140$ for $\theta = \frac{\pi}{6}$.

For the rest of this subsection, the vertex space of $\Gamma = 0$ is obtained using the constructive geometric approach. As each limb is constituted of two moving links thus their corresponding motions are shown respectively in Figs. 8 and 9. Skipping mathematical details, the equations for the circles and lines in Fig. 8 are:

$$(z' - w'_{iz} \pm \frac{\Delta\rho_i}{2}\sin\theta)^2 + (x' - w'_{ix} \pm \frac{\Delta\rho_i}{2}\cos\theta)^2 = l_{1i^2} \quad (19)$$

$$z'\sin\theta + x'\cos\theta = w_{ix} \pm l_{1i} \quad (20)$$

For a given x', solving z' from above, called z'_{bj}, $j = 1, 2$, leads to

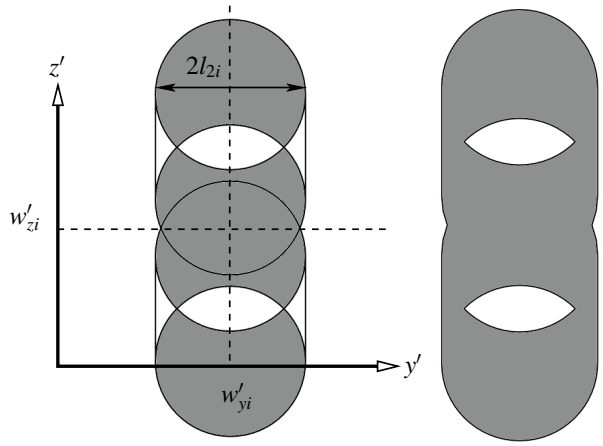

Figure 9. BOUNDARY GENERATED BY THE SECOND MOVING LINK FOR $\Gamma = 0$ DUE TO THE FIRST MOVING LINK.

the following circles and lines which are depicted in Fig. (9):

$$ {}^0\mathcal{L}_i : (z' - z'_{bj})^2 + (y' - w'_{iy})^2 = l_{2i}^2 \tag{21} $$

$$ {}^0\mathcal{C}_i : y' = w'_{iy} \pm l_{2i} \tag{22} $$

The intervals for which includes the vertex space are:

$$ \lim_{\min i} x : w'_{ix} - l_{1i} - \frac{\Delta\rho_i}{2}|\sin\theta| \leq x'_h \leq w'_{ix} + l_{1i} + \frac{\Delta\rho_i}{2}|\sin\theta| : \lim_{\max i} x \tag{23} $$

$$ w'_{iy} - l_{2i} \leq y'_H \leq w'_{iy} + l_{2i} \tag{24} $$

$$ w'_{iz} - l_{1i} - \frac{\Delta\rho_i}{2}|\cos\theta| \leq z'_h \leq w'_{ix} + l_{1i} + \frac{\Delta\rho_i}{2}|\cos\theta| \tag{25} $$

Using the same reasoning explained previously for $\Gamma = 1$, the problem of obtaining the vertex space for $\Gamma = 0$ is made equivalent to finding the intersections of two pairs of two circles connect by two lines, Eqn. (21) and (22), for a given $\mathcal{X}$ cross section and identifying which arc or line is constituting the boundary of the vertex space. This can be done by having in mind the reasoning provided above for $\Gamma = 1$: checking the boundary condition for the chosen point and also using the algorithm presented in [17]. Since a CAD model is presented for the vertex space of $\Gamma = 0$, Fig. 7, thus the vertex space obtained by using the above procedure is omitted.

3.2 Constant-orientation Workspace

Several methods are presented in the literature for the determination of the constant-orientation of a parallel mechanism. However the great majority of these approaches rely on the idea to intersect the vertex space of each limb either by a CAD software or by obtaining the geometrical expression of the vertex space and implement into a computer algebra system. An elaborated survey about the advantages and drawbacks of both approaches can be found in [20]. The analysis of the vertex space

i	$(\mathbf{r}_i)_x$	$(\mathbf{r}_i)_y$	$(\mathbf{r}_i)_z$	$(\mathbf{s}'_i)_x$	$(\mathbf{s}'_i)_y$	$(\mathbf{s}'_i)_z$
1	140	0	70	0	-30	30
2	140	70	0	30	0	0
3	70	140	0	0	30	0
4	0	70	0	-30	0	0
5	0	140	70	0	30	30

Table 1. GEOMETRIC PROPERTIES (IN MM) ASSUMED FOR THE 5-PRUR PARALLEL MECHANISM.

in the preceding sections is arranged in such a way that allows to obtain the constant-orientation workspace using both approaches mentioned above. Having in place the CAD model of the vertex space we are one step away from the CAD model of the constant-orientation workspace. The final step is to apply an offset vector to all the five vertex spaces which is in opposite direction of the vector connecting the last joint of the limb to the mobile frame attached to the platform, $\mathbf{s}_i$. Finally, the workspace will be the intersection of the five offsetting vertex spaces. Figure 10(a) illustrates the CAD model of the constant-orientation workspace for a given orientation of the platform. Emphasis in this section is placed on geometrical construction of the constant-orientation workspace which is inspired from the algorithm presented in [17] which was also used above for the geometrical construction of the vertex space. The foregoing algorithm is not fully developed here and only some primordial issues are presented which should be inevitably considered in order to find the constant-orientation workspace of a 5-PRUR parallel mechanism. The first step is to reduce the three-dimensional space to two-dimensional one using the cross section plane $\mathcal{X}$ defined in Eqn. (12). As pointed out previously, Eqn. (12) results in homogeneous sections for $\mathcal{X}$ which are constituting of some circles and lines. Consider a 5-PRUR comprising $\mathfrak{g}$ limb having $\Gamma = 0$ and $5 - \mathfrak{g}$ limb with $\Gamma = 1$. The set of all the circles and lines obtained by applying the cross section plane $\mathcal{X}$ for the five vertex spaces is defined respectively as $\mathcal{C}$ and $\mathcal{L}$:

$$ \mathcal{C} = \{{}^0\mathcal{C}_1, \ldots, {}^0\mathcal{C}_\mathfrak{g}, {}^1\mathcal{C}_1, \ldots, {}^1\mathcal{C}_{\mathfrak{g}-5}\} \tag{26} $$

$$ \mathcal{L} = \{{}^0\mathcal{L}_1, \ldots, {}^0\mathcal{L}_\mathfrak{g}, {}^1\mathcal{L}_1, \ldots, {}^1\mathcal{L}_{\mathfrak{g}-5}\} \tag{27} $$

The cross section $\mathcal{X}$ is repeated along x' axis, x'_H, over the following interval:

$$ \max\left\{\lim_{\min i} x\right\} \leq x'_H \leq \min\left\{\lim_{\max i} x\right\}, \quad i = 1, \ldots, 5 \tag{28} $$

In the above, $\lim_{\min i} x$ and $\lim_{\max i} x$ were defined in Eqs. (16) and (23) for $\Gamma = 1$ and $\Gamma = 0$, respectively. Having in place all the infor-

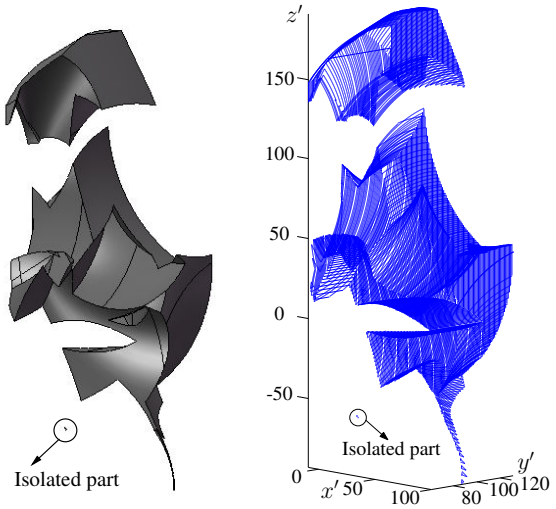

(a) CAD model (b) Geometrical constructive approach

Figure 10. CONSTANT-ORIENTATION WORKSPACE FOR $\theta = \frac{\pi}{6}$ AND $\phi = \frac{\pi}{3}$ FOR THE DESIGN PRESENTED IN TABLE1.

mation concerning the circles (centre and radius) and lines (expression) from Eqs. (26) and (27) and considering the required interval for applying the cross section, the following steps should be followed in order to find the constant-orientation workspace:

1. Finding the intersection points of all the circles in $\mathcal{C}$;
2. Finding the intersection points of circles, $\mathcal{C}$, with lines,$\mathcal{L}$;
3. Finding the intersection points between lines, $\mathcal{L}$;
4. Ordering the intersection points found above. (Hint: The intersection points of circles are ordered using atan2 function and intersection point of lines in ascending order);
5. Determining each arc or line constituting the boundary of the constant-orientation workspace.

The last item is the most challenging part and it should be elaborated with care. To do so, one should verify whether a given point, preferably the mid-points, belonging to the arc or line is inside of all the vertex spaces. To do so, the mid-point of the arc or line is considered and substituted into the IKP of all the limbs. Obviously, the arc or line will be a boundary of the workspace if the mid-point satisfies the boundary condition, i.e. the IKP inequality constraint, and the strokes of all the actuators. Figures 10(b) represent the constant-orientation workspace for given rotation angles of the platform. The constant-orientation workspace obtained by the CAD software, Fig. 10(a), is coherent with the one obtained by implementing the geometrical constructive approach in a computer algebra system, Fig. 10(b). As it can be observed form the latter two figures, the constant-orientation workspace is highly irregular and also may have an extremely small isolated part which is usually unexpected.

As elaborated in [17], reaching this step the volume of the constant-orientation workspace can be obtained. The technique is essentially based on the *Gauss Divergence Theorem* which can be applied to planar regions. As mentioned previously, the constant-orientation workspace for a given cross section consists of the intersection of circles, resulting in some arcs, and lines. Thus, in order to compute the area, $\mathcal{D}_i$, for a given section the area created by both arcs and lines should be considered. Based on results obtained in [17], apart from some minor modifications, the area created by an outer-arc— with centre of curvature as $[h,g]^T$, its radius of curvature r and the angle corresponding to the end points θ_1 and θ_2, (not to be confused with θ for DOF)— can be written as:

$$\mathcal{D}_i = hr[\sin\theta_2 - \sin\theta_1] + gr[\cos\theta_1 - \cos\theta_2] + r^2[\theta_2 - \theta_1]. \quad (29)$$

In what concerns the area created by the lines based on the formulation given in [17] for the *Gauss Divergence Theorem*, upon performing the integration, for the outer lines, it follows that :

$$\mathcal{D}_i = \begin{cases} -y'_l(z'_u - z'_l) & \text{vertical line located in the left side of} w'_{iy} \\ y'_r(z'_u - z'_l) & \text{vertical line located in the right side of} w'_{iy} \\ -z'_l(y'_r - y'_l) & \text{horizontal line located in the lower side of} w'_{iz} \\ z'_u(y'_r - u'_l) & \text{horizontal line located in the upper side of} w'_{iy} \end{cases} \quad (30)$$

where (z'_l, z'_u) and (y'_r, y'_l) stand respectively for the z' (lower and upper) and y' (right and left) components of the line constituting the boundary of the constant–orientation workspace found by the algorithm. For the inner lines and arcs the negative values of $\mathcal{D}_i$ should be considered. Finally, the area of the workspace is $\frac{1}{2}\sum \mathcal{D}_i$. The above formulation for computing the volume of the workspace is integrated inside the algorithm for obtaining the boundary of the constant-orientation workspace. Figure 11 represent the volume of the constant-orientation workspace with respect of two permitted orientations, (ϕ, θ), for the designs presented in Table (1).

4 CONCLUSION

This paper investigated the constant-orientation workspace of 5-DOF parallel mechanisms (3T2R) with a limb kinematic arrangement of type PRUR. From the results for the IKP, two types of 5-PRUR limbs were presented, $\Gamma = 0$ and $\Gamma = 1$, whose IKP and the vertex spaces are completely different. Bohemian domes appeared in the geometrical interpretation of each limb and led to a CAD representation of the constant-orientation workspace. An algorithm was proposed in order to find the boundary of the vertex space and the constant-orientation workspace which can be implemented in any computer algebra system. The algorithm made it possible to find the volume of the constant-orientation

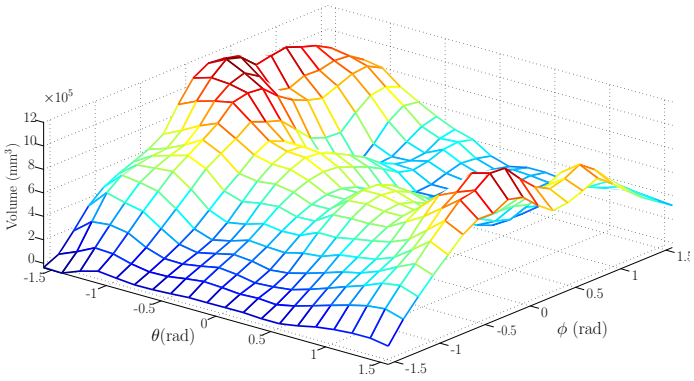

Figure 11. VOLUME OF THE CONSTANT-ORIENTATION WITH RESPECT OF (ϕ, θ) FOR THE DESIGN PRESENTED IN TABLE 1.

workspace by applying the *Gauss Divergence Theorem* and provided some insight into the optimum synthesis of 5-PRUR parallel mechanisms. ongoing works include the optimum design of such mechanisms with regard to the singular barriers.

ACKNOWLEDGMENT

The authors would like to acknowledge the financial support of the Natural Sciences and Engineering Research Council of Canada(NSERC) as well as the Canada Research Chair program.

REFERENCES

[1] Davidson, J. K., and Hunt, K. H., 2004. *Robots and Screw Theory*. Oxford University Press.

[2] "Parallelmic, http://www.parallemic.org/".

[3] Kong, X., and Gosselin, C., 2007. *Type Synthesis of Parallel Mechanisms*, Vol. 33. Springer, Heidelberg.

[4] Huang, Z., and Li, Q. C., 2002. "General Methodology for Type Synthesis of Symmetrical Lower-Mobility Parallel Manipulators and Several Novel Manipulators". *The International Journal of Robotics Research,* **21**(2), pp. 131–145.

[5] Fang, Y., and Tsai, L. W., 2002. "Structure Synthesis of a Class of 4-DoF and 5-DoF Parallel Manipulators with Identical Limb Structures". *The International Journal of Robotics Research,* **21**(9), pp. 799–810.

[6] Huang, Z., and Li, Q. C., 2003. "Type Synthesis of Symmetrical Lower-Mobility Parallel Mechanisms Using the Constraint–Synthesis Method". *The International Journal of Robotics Research,* **22**(1), pp. 59–79.

[7] Kong, X., and Gosselin, C., 2005. "Type Synthesis of 5-DOF Parallel Manipulators Based on Screw Theory". *Journal of Robotic Systems,* **22**(10), pp. 535–547.

[8] Zhu, S. J., and Huang, Z., 2007. "Eighteen Fully Symmetrical 5-DoF 3R2T Parallel Manipulators with Better Actuating Modes". *The International Journal of Advanced Manufacturing Technology,* **34**(3), pp. 406–412.

[9] Wang, J., and Gosselin, C., 1997. "Kinematic Analysis and Singularity Representation of Spatial Five-Degree-of-Freedom Parallel Mechanisms". *Journal of Robotic Systems,* **14**(12), pp. 851–869.

[10] Mbarek, T., Barmann, I., and Corves, B., 2004. "Fully Parallel Structures with Five Degree of Freedom: Systematic Classification and Determination of Workspace". In Proceedings Mechatronics & Robotics, pp. 990–995.

[11] Gao, F., Peng, B., Zhao, H., and Li, W., 2006. "A Novel 5-DOF Fully Parallel Kinematic Machine Tool". *The International Journal of Advanced Manufacturing Technology,* **31**(1), pp. 201–207.

[12] T. Masouleh, M., and Gosselin, C. "Singularity Analysis of 5-RPRRR Parallel Mechanisms via Grassmann Line Geometry". In Proceedings of the 2009 ASME Design Engineering Technical Conferences, DETC2009-86261.

[13] Zhu, S. J., Huang, Z., and Zhao, M. Y., 2007. "Singularity Analysis for a 5-DoF Fully-Symmetrical Parallel Manipulator 5-RRR (RR)". In IEEE International Conference on Robotics and Automation, pp. 1189–1194.

[14] Zhu, S., Huang, Z., and Zhao, M., 2009. "Singularity analysis for six practicable 5-DoF fully-symmetrical parallel manipulators". *Mechanism and Machine Theory,* **44**(4), pp. 710–725.

[15] Zhu, S. J., Huang, Z., and Zhao, M. Y., 2008. "Kinematics of a Partially Decoupled 3R2T Symmetrical Parallel Manipulator 3-RCRR". *Proceedings of the Institution of Mechanical Engineers, Part C: Journal of Mechanical Engineering Science,* **222**(2), pp. 277–285.

[16] Merlet, J. P., 2006. *Parallel Robots* . Springer.

[17] Gosselin, C., 1990. "Determination of the Workspace of 6-DOF Parallel Manipulators". *ASME Journal of Mechanical Design,* **112**(3), pp. 331–336.

[18] Bonev, I. A., and Gosselin, C. M., 2002. "Geometric Algorithms for the Computation of the Constant-Orientation Workspace and Singularity Surface of a Special 6-RUS Parallel Manipulator". In Proceedings of the 2000 ASME Design Engineering Technical Conferences, DETC2002/MECH-34257.

[19] Gosselin, C., Masouleh, M. T., Duchaine, V., Richard, P. L., Foucault, S., and Kong, X., 2007. "Parallel Mechanisms of the Multipteron Family: Kinematic Architectures and Benchmarking". In IEEE International Conference on Robotics and Automation, pp. 555–560.

[20] Bonev, I. A., 2002. "Geometric Analysis of Parallel Mechanisms". PhD thesis, Laval University, Quebec, QC, Canada, October.